

# Characteristic vibrational modes of a single vacancy in a zigzag carbon nanotube

H. Y. He and B. C. Pan

Hefei National Laboratory for Physical Sciences at Microscale and Department of Physics, University of Science and Technology of China, Hefei, Anhui 230026, People's Republic of China

(Received 10 September 2007; published 27 February 2008)

We have applied *ab initio* calculations to studying phonon frequencies and the corresponding eigenmodes for zigzag carbon nanotubes with single vacancies. We find two types of vibrational modes that serve as fingerprints of the single vacancy, which may be detected by Raman spectra technique. Our calculations reveal that these vibrational frequencies exhibit a weak size dependence on the diameters of tubes. Moreover, it is found that the frequencies of radial breathing modes of the defective tubes are quite close to those of the related perfect ones.

DOI: [10.1103/PhysRevB.77.073410](https://doi.org/10.1103/PhysRevB.77.073410)

PACS number(s): 61.72.J-, 63.22.-m, 61.46.Fg, 71.15.Mb

## I. INTRODUCTION

Carbon nanotubes (CNTs) have been extensively studied due to their unique mechanical, electrical, and chemical properties.<sup>1-5</sup> Meanwhile, many efforts have been devoted both theoretically and experimentally to the study of the lattice dynamics of CNTs, one of fundamental properties.<sup>6-14</sup> Essentially, the vibrational properties are closely coupled with the atomic structure of a system. For a perfect carbon nanotube, it was found that the frequency of a radial breathing mode (RBM), a special mode in which all atoms subject to radial displacement, is inversely proportional to the radius and independence of the chirality of a tube.<sup>7,11</sup> While the atomic structure of a perfect tube is altered, which may result from deformation or structural defects, the vibrational properties of the tube are certainly influenced. Up to date, the vibrational features of deformed tubes have been reported by many researchers. For example, using tight-binding molecular dynamics, Dereli *et al.* revealed that the vibrational frequencies of CNTs in radial direction decrease sensitively with increasing strain rate.<sup>15</sup> Cao *et al.* found that the vibrational characteristics of the carbon nanotube is very sensitive to small axial stains, and tubes with smaller radii have higher sensitivities.<sup>16</sup> Based on *ab initio* calculations, it was reported that both frequencies and intensities of the low-frequency Raman-active modes almost did not change in the deformed nanotubes by uniaxial and torsional strains, while their high-frequency part shifted significantly.<sup>17</sup>

On the other hand, structural defects in CNTs, such as single vacancies and Stone-Wales (SW) defects, which can be generated during the growth,<sup>18</sup> surely affect the vibrational properties, too. Miyamoto *et al.* identified the SW defects in carbon nanotubes by combining resonant photoabsorption and vibration spectroscopy with scanning tunneling microscopy and time dependent density functional calculations.<sup>19</sup> They found that a vibrational frequency of 1962 cm<sup>-1</sup> served as a fingerprint of such a defect in the CNT. In addition, the Raman spectra of the topological defects of the carbon nanotube containing pentagon and heptagon rings were also studied.<sup>20</sup> However, vibrational modes related to an individual single vacancy, a very simple and common structural defect in CNTs,<sup>21-24</sup> have not been reported to the best of our knowledge.

In this paper, we systematically investigate the vibrational modes of zigzag nanotubes ( $n,0$ ) ( $n$  varying from 7–9) with a single vacancy, using the frozen phonon approach within local density approximation (LDA) calculations. We find two kinds of vibrational modes caused by the existed single vacancy in CNTs, which weakly couple with the radius of the tube. Both of the modes are Raman active, predicted by the empirical bond polarizability model. These modes can serve as indicators of a single vacancy in a CNT.

## II. COMPUTATIONAL METHOD

Our calculations are performed using the first principles self-consistent pseudopotential program known as SIESTA,<sup>25</sup> which is within the framework of LDA. A double- $\zeta$  basis set<sup>26</sup> is used for the localized basis orbitals of C atoms. The carbon nanotubes ( $n,0$ ) ( $n=7-9$ ) containing a single vacancy together with the related perfect tubes are chosen in our calculations. For each tube, a periodic boundary condition along the tube axis is used, and the supercell length in the tube axis is 25.56 Å, which is large enough to neglect the interaction between the images of the single vacancies in CNTs.

The systems under consideration are fully optimized using the above mentioned approach, so that the maximum force acting on each atom is less than 0.02 eV/Å. In our optimization, a single  $k$  point (at  $\Gamma$ ) is used to sample the Brillouin zone because the supercells chosen by us are large enough. These relaxed geometries are used as the starting structures for the phonon calculation. In our phonon calculation, we employ the frozen phonon approximation.<sup>27</sup> That is, the force constant  $C_{i,\alpha;j,\beta}$  is derived from the numerical derivatives of the force versus displacements of  $\Delta_{j,\beta}$ :

$$C_{i,\alpha;j,\beta} = -\frac{F_{i,\alpha}}{\Delta_{j,\beta}}. \quad (1)$$

Here,  $i$  and  $j$  stand for the labels of atoms, and  $\alpha$  and  $\beta$  refer to the direction (say,  $x$ ,  $y$ , or  $z$ ). The force  $F_{i,\alpha}$  of  $i$ th atom in the direction  $\alpha$  is caused by the displacement of  $j$ th atom in the direction of  $\beta$ . We set each atom in a system to displace away by 0.04 Bohr along  $\pm x$ ,  $\pm y$ , and  $\pm z$  directions from its equilibrium position, respectively. According

to the calculations, the force constants in  $x$ ,  $y$ , or  $z$  direction are obtained by average of the force constants referring to  $\pm x$ ,  $\pm y$ , or  $\pm z$ . These force constants are used to build up the dynamical matrix of the system.<sup>28</sup> By solving the equation

$$-\omega^2 M_i u_{i,\alpha} = -\sum_{j,\beta} C_{i,\alpha,j,\beta} u_{j,\beta}, \quad (2)$$

the vibrational frequencies  $\omega$  and the corresponding eigenmodes  $u_{i,\alpha}$  are yielded, where  $M_i$  is the mass of  $i$ th atom.

### III. RESULTS AND DISCUSSIONS

As we know, a single atomic vacancy is formed by removing a single carbon atom from a carbon nanotube, leaving three dangling bonds (DBs) behind. In general, the adjacent DBs at the single vacancy are unstable. When the size of a CNT is not large enough, two of three DBs will rebond with each other to form a new C–C bond, leaving a DB there. Thus, an ideal single vacancy is converted to a configuration consisting of a pentagon and a dangling bond atom, so-called 5-1DB defect.<sup>22</sup> By performing full relaxation, the formation energies of single vacancies in the chosen tubes are predicted to be 5.5, 5.7, and 5.8 eV for (7,0), (8,0) and (9,0) respectively, which are comparable with those calculated from the tight-binding method.<sup>22</sup>

For a tube containing individual single vacancies, the atomic structure around the defects in the tube is quite different from that of the perfect portion. Our calculation finds that the single vacancy in each carbon nanotube mainly distorts the local structure of about three atomic shells around it, being consistent with the previous report.<sup>22</sup> So, if the density of the single vacancies in a tube is very low, the perturbation of the structure arising from a vacancy is quite localized.

In order to reveal the vibration properties of a CNT influenced by a single vacancy, we first explore the vibrational frequencies and the related eigenmodes of perfect (7,0), (8,0), and (9,0) CNTs, respectively, with the frozen phonon method. By examining the obtained eigenmodes, we identify the radial breathing modes for the tubes, and find the RBM frequencies for these tubes emerge at 433.7, 365.3, and 332.6  $\text{cm}^{-1}$ , respectively, of which the RBM frequency of (9,0) tube is well consistent with that (329  $\text{cm}^{-1}$ ) reported before.<sup>29</sup> Moreover, the coefficient of  $A$  ( $\omega_{\text{RBM}} = A/R$ ,  $R$  is the tube radius in Å.) obtained from our calculation is quite close to the reported value,<sup>29</sup> too.

Then we deal with the vibrational properties of the defected carbon nanotubes. From the calculated eigenmodes, we observe a special vibrational mode, in which displacements of C atoms are all in radial direction with different amplitudes, for each defected tube. These RBM-like mode positions are found at 433.8, 369.4, and 314.7  $\text{cm}^{-1}$  for the tubes of  $n=7-9$ , respectively, differing by only about 10  $\text{cm}^{-1}$  from the related RBM frequencies of the perfect tubes. Moreover, the major features of some vibrational modes existed in the perfect carbon nanotube almost remain in the tube with a single vacancy. This is essentially due to the fact that the 5-1DB defect is quite localized.

In addition to these vibrational modes as mentioned above, we pay more attention to the vibrational modes asso-

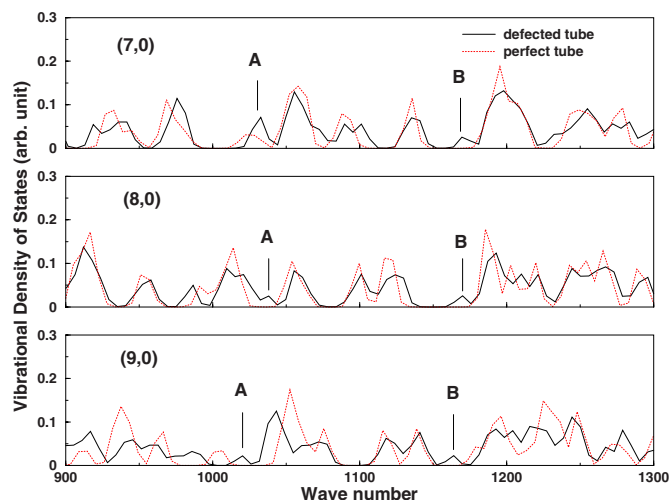


FIG. 1. (Color online) The VDOS of the concerned defected tubes and their related perfect tubes. The modes marked A and B indicate two concerned modes.

ciated with the 5-1DB defect. Figure 1 plots the calculated vibrational density of states (VDOS) for the defected tubes and the related perfect tubes. From Fig. 1, we not only find that the VDOS of the perfect tubes is perturbed by a single vacancy but also observe some vibrational frequencies of the defected tubes present in the gaps of the vibrational frequencies of the perfect ones. Carefully examining the eigenmodes related to these frequencies, we find that two types of typical vibrational patterns appear in each of the defected tubes, and the frequencies of these modes are marked with A and B, respectively in Fig. 1. Clearly, the frequencies marked with A are 1028.6, 1036.5, and 1019.5  $\text{cm}^{-1}$ , and the frequencies marked with B are 1170.1, 1168.1, and 1163.8  $\text{cm}^{-1}$ , for tubes  $(n,0)$  with  $n$  ranging from 7 to 9, respectively. These frequencies vary only slightly with radii of the tubes, which implies that they are not sensitive to the size of the tube. For both types of vibrational modes, the common character is that the amplitudes of the displacements of atoms subject to the single vacancy are the largest, while those of the atoms being far away from the defect become much smaller. Moreover, the amplitudes of the displacements of the C atoms around 5-1DB are not uniform. Some atoms at the vacancy have significantly larger displacements than other atoms. Hence, these modes localize at the 5-1DB defect somewhat. These two kinds of vibrational patterns around the vacancy are plotted in Fig. 2, where the arrows attached at atoms represent the direction and amplitude of the atom displacement. Obviously, in mode A [shown in Fig. 2(a)], two atoms of both C1 and C2, nearest to DB atom in pentagon, subject to the largest amplitude of their displacements, whereas C3 with a slight displacement. For mode B, as shown in Fig. 2(b), C1, C2, and DB atom deviate from their equilibrium positions to the void or in a reverse direction. Meanwhile, C3 and two neighboring atoms of DB atom make a certain contribution to this mode. The observations above strongly indicate that both modes A and B, which are induced by a single vacancy, can be regarded as the identification of the 5-1DB defect.

Note that all calculations above are performed at the LDA level. To assess the validity of our results from LDA calcu-

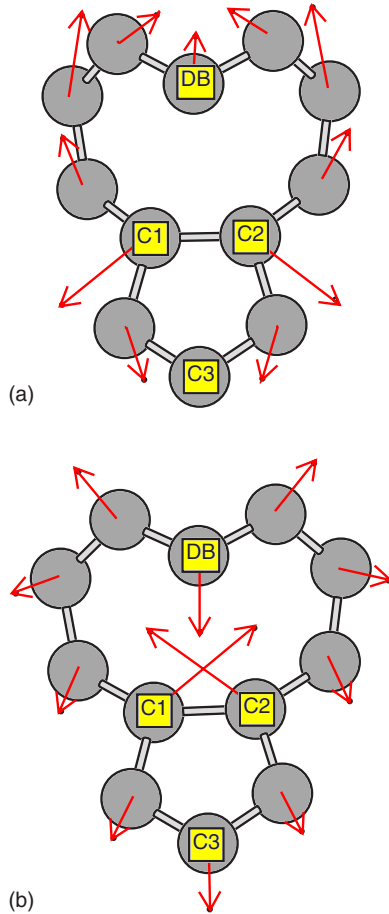


FIG. 2. (Color online) The local vibrational features near the 5-1DB defect in a (7,0) tube for (a) mode A; and (b) mode B. The relevant atoms are labeled.

lation, we recalculate the vibrational properties of (7,0) carbon nanotube with or without a single vacancy at the level of the Perdew-Burke-Ernzerhof generalized gradient approximation (GGA).<sup>30</sup> Meanwhile, a single vacancy in a graphene sheet is also handled for comparison between the two levels of LDA and GGA. The calculated formation energy of the single vacancy in the graphene consisting of 160 atoms is predicted to be about 8.3 eV at the level of GGA, which is consistent with the previous reported GGA value,<sup>31</sup> but lower by about 0.4 eV than that of LDA. For the case of (7,0) tube, the formation energy of a single vacancy evaluated from GGA calculation is also lower than that from the LDA calculation by less than 0.3 eV. Therefore, our results show that the formation energy of a single atomic vacancy from GGA calculation is systematically lower than that from LDA calculation. According to the frozen phonon calculation, the frequencies obtained from GGA shift downward by 50  $\text{cm}^{-1}$  with respect to the corresponding ones from LDA. Especially, the RBM for the perfect (7,0) tube and the RBM-like mode for the defected (7,0) tube that appear at 418.5 and 422.9  $\text{cm}^{-1}$ , respectively, shift downward by less than 15  $\text{cm}^{-1}$  with respect to those from LDA calculation. In addition, the frequencies for modes A and B of the single vacancy in (7,0) CNT locate at 1008.9 and 1151.2  $\text{cm}^{-1}$ , respectively, quite close to the values from the LDA

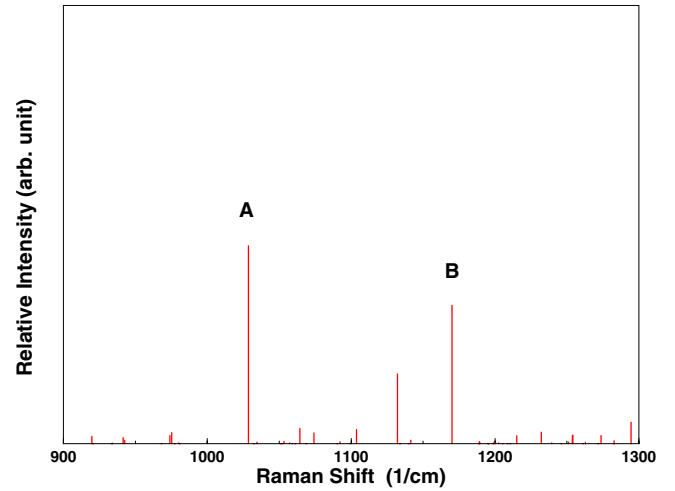


FIG. 3. (Color online) Relative Raman intensity of mode A and mode B for (7,0) carbon nanotube.

calculations. These tests show that although the formation energy of the vacancy obtained from LDA is higher than that from GGA, the difference of the vibrational frequencies evaluated from LDA and GGA is not significant yet. So the reported vibrational characteristics of the single vacancy in a CNT from the LDA calculation as mentioned above is valid.

Before closing this paper, we extend our study to the Raman spectra of the defective tubes. Usually, the existence of structural defects in a CNT lowers the symmetry of the tube, resulting in more Raman-active modes. For our concerned systems, we calculate the Raman intensity for all phonon modes using the empirical bond polarizability model<sup>11,32</sup> at a phonon temperature of 300 K, with a laser excitation wavelength of 514.5 nm. Our calculations show that the Raman intensity of the RBM-like mode is the strongest of all modes, and the concerned modes A and B for each tube are also Raman active. Moreover, the intensities of both modes A and B are observed to be stronger than the others in the frequency range of 900–1300  $\text{cm}^{-1}$ ; a typical case for (7,0) tube was displayed in Fig. 3. According to the analysis above, we propose that the single vacancies in CNTs can probably be probed via detecting the signals of modes A and B in Raman spectra.

#### IV. CONCLUSIONS

In this work, the vibrational modes of some zigzag CNTs with a single vacancy are investigated based on *ab initio* calculations. Two types of modes are identified as the characteristic vibration of a single vacancy. In addition, RBM-like modes are found for the defected tubes, the frequencies of which just make a little shift with respect to RBM frequencies of the related perfect ones. Furthermore, using the empirical bond polarizability model, the nonresonant Raman spectra of these defected tubes are calculated. The RBM-like mode for each tube causes the most intensive Raman spectrum, and two types of characteristic vibrational modes of a single vacancy are both Raman active.

## ACKNOWLEDGMENTS

This work was partially supported by the Fund of the University of Science and Technology of China, the Fund of

the Chinese Academy of Science, and by the NSFC Grant Nos. 50121202, 60444005, and 10574115. This work was partially supported by the National Basic Research Program of China, Grant No. 2006CB922000.

- 
- <sup>1</sup>H. Dai, J. H. Hafner, A. G. Rinzler, D. T. Colbert, and R. E. Smalley, *Nature (London)* **384**, 147 (1996).  
<sup>2</sup>P. Kim and C. M. Lieber, *Science* **286**, 2148 (1999).  
<sup>3</sup>P. Pancharal, Z. L. Wang, D. Ugarte, and W. de Heer, *Science* **283**, 1513 (1999).  
<sup>4</sup>S. J. Tans, R. M. Verschueren, and C. Dekker, *Nature (London)* **393**, 49 (1999).  
<sup>5</sup>R. S. Friedman, N. C. McAlpine, D. S. Ricketts, D. Ham, and C. M. Lieber, *Nature (London)* **434**, 1085 (2005).  
<sup>6</sup>M. S. Dresselhaus and P. C. Eklund, *Adv. Phys.* **49**, 705 (2000).  
<sup>7</sup>A. M. Rao, E. Richter, S. Bandow, B. Chase, P. C. Eklund, K. W. Williams, M. Menon, K. R. Subbaswamy, A. Thess, R. E. Smalley, G. Dresselhaus, and M. S. Dresselhaus, *Science* **275**, 187 (1997).  
<sup>8</sup>A. Kasuya, Y. Sasaki, Y. Saito, K. Tohji, and Y. Nishina, *Phys. Rev. Lett.* **78**, 4434 (1997).  
<sup>9</sup>J. Hone, B. Batlogg, Z. Benes, A. T. Johnson, and J. E. Fischer, *Science* **289**, 1730 (2000).  
<sup>10</sup>R. A. Jishi, L. Venkataraman, M. S. Dresselhaus, and G. Dresselhaus, *Chem. Phys. Lett.* **209**, 77 (1993).  
<sup>11</sup>R. Saito, T. Takeya, T. Kimura, G. Dresselhaus, and M. S. Dresselhaus, *Phys. Rev. B* **57**, 4145 (1998).  
<sup>12</sup>R. Saito, T. Takeya, T. Kimura, G. Dresselhaus, and M. S. Dresselhaus, *Phys. Rev. B* **59**, 2388 (1999).  
<sup>13</sup>V. P. Sokhan, D. Nicholson, and N. Quirke, *J. Chem. Phys.* **113**, 2007 (2000).  
<sup>14</sup>D. Kahn and J. P. Lu, *Phys. Rev. B* **60**, 6535 (1999).  
<sup>15</sup>G. Dereli and C. Ozdogan, *Phys. Rev. B* **67**, 035416 (2003).  
<sup>16</sup>G. X. Cao, X. Chen, and J. W. Kysar, *Phys. Rev. B* **72**, 195412 (2005).  
<sup>17</sup>G. Wu, J. Zhou, and J. M. Dong, *Phys. Rev. B* **72**, 115411 (2005).  
<sup>18</sup>D. B. Mawhinney, V. Naumenko, A. Kuznetsova, J. T. Yates, Jr., J. Liu, and R. E. Smalley, *Chem. Phys. Lett.* **324**, 213 (2000).  
<sup>19</sup>Y. Miyamoto, A. Rubio, S. Berber, M. Yoon, and D. Tomanek, *Phys. Rev. B* **69**, 121413(R) (2004).  
<sup>20</sup>G. Wu, and J. M. Dong, *Phys. Rev. B* **73**, 245414 (2006).  
<sup>21</sup>P. M. Ajayan, V. Ravikumar, and J. C. Charlier, *Phys. Rev. Lett.* **81**, 1437 (1998).  
<sup>22</sup>A. J. Lu and B. C. Pan, *Phys. Rev. Lett.* **92**, 105504 (2004).  
<sup>23</sup>A. V. Krashenninnikov, K. Nordlund, M. Sirvio, E. Salonen, and J. Keinonen, *Phys. Rev. B* **63**, 245405 (2001).  
<sup>24</sup>S. Zhang, S. Mielke, R. Khare, D. Troya, R. Ruoff, G. Schatz, and T. Belytschko, *Phys. Rev. B* **71**, 115403 (2005).  
<sup>25</sup>D. Sanchez-Portal, P. Ordejon, E. Artacho, and J. M. Soler, *Int. J. Quantum Chem.* **65**, 453 (1997); N. Troullier and J. L. Martins, *Phys. Rev. B* **43**, 1993 (1991).  
<sup>26</sup>J. M. Soler, E. Artacho, J. D. Gale, A. Garcia, J. Junquera, P. Ordejon, and D. Sanchez-Portal, *J. Phys.: Condens. Matter* **14**, 2745 (2002), and references therein.  
<sup>27</sup>M. T. Yin and M. L. Cohen, *Phys. Rev. B* **26**, 3259 (1982).  
<sup>28</sup>To obtain accurate VDOS, five  $k$  points were employed in each dynamical matrix.  
<sup>29</sup>J. Kurti, G. Kresse, and H. Kuzmany, *Phys. Rev. B* **58**, R8869 (1998).  
<sup>30</sup>J. P. Perdew, K. Burke, and M. Ernzerhof, *Phys. Rev. Lett.* **77**, 3865 (1996).  
<sup>31</sup>L. Li, S. Reich, and J. Robertson, *Phys. Rev. B* **72**, 184109 (2005).  
<sup>32</sup>S. Guha, J. Menendez, J. B. Page, and G. B. Adams, *Phys. Rev. B* **53**, 13106 (1996).